



## Molecular Crystals and Liquid Crystals Incorporating Nonlinear Optics

Publication details, including instructions for authors and  
subscription information:

<http://www.tandfonline.com/loi/gmcl17>

### Steady-State vs. Pulsed Excitation Recombination Kinetics: Simulations and Experiments on Pores, Powders and Random Media

S. J. Parus<sup>a</sup> & R. Kopelman<sup>a</sup>

<sup>a</sup> Department of Chemistry, University of Michigan, Ann Arbor,  
MI, 48109, U.S.A.

Version of record first published: 22 Sep 2006.

To cite this article: S. J. Parus & R. Kopelman (1989): Steady-State vs. Pulsed Excitation  
Recombination Kinetics: Simulations and Experiments on Pores, Powders and Random Media,  
Molecular Crystals and Liquid Crystals Incorporating Nonlinear Optics, 175:1, 119-134

To link to this article: <http://dx.doi.org/10.1080/00268948908033750>

PLEASE SCROLL DOWN FOR ARTICLE

Full terms and conditions of use: <http://www.tandfonline.com/page/terms-and-conditions>

This article may be used for research, teaching, and private study purposes. Any  
substantial or systematic reproduction, redistribution, reselling, loan, sub-licensing,  
systematic supply, or distribution in any form to anyone is expressly forbidden.

The publisher does not give any warranty express or implied or make any  
representation that the contents will be complete or accurate or up to date. The  
accuracy of any instructions, formulae, and drug doses should be independently  
verified with primary sources. The publisher shall not be liable for any loss, actions,  
claims, proceedings, demand, or costs or damages whatsoever or howsoever caused  
arising directly or indirectly in connection with or arising out of the use of this material.

# Steady-State vs. Pulsed Excitation Recombination Kinetics: Simulations and Experiments on Pores, Powders and Random Media

S. J. PARUS and R. KOPELMAN

*Department of Chemistry, University of Michigan, Ann Arbor, MI 48109, U.S.A.*

*(Received October 20, 1988)*

The non-classical kinetics of exciton recombination in restricted geometries provides the foundation for a new experimental technique of probing the exciton dynamics and the sample topology. The phosphorescence and delayed fluorescence decays exhibit a dramatic dependence on the duration of the excitation. The comparison of pulsed and steady-state excitation provides information on the local topology of the sample and on the average hopping time of the exciton and the exciton diffusion length. This is possible because the distribution of the exciton population is non-Poissonian under steady-state excitation conditions. In addition, the pulse-created distribution also loses its Poissonian character with time. The experimental systems are: 1) Isotopic mixed naphthalene crystals above and below percolation; 2) Naphthalene crystalline powder; 3) Naphthalene embedded into porous glass. Except for the mixed crystals above the percolation concentration, all samples exhibit the non-classical effects. The interpretation is aided by Monte-Carlo simulations on: 1) Cubic lattice; 2) Three-dimensional percolation clusters; 3) Three-dimensional islands; 4) The fractal Menger "sponge"; 5) Square lattice; 6) Two-dimensional percolation clusters; 7) Sierpinski "carpet" and "gasket"; 8) One-dimensional lattice; 9) One-dimensional islands. The porous glass data are only consistent with the one-dimensional island model.

## INTRODUCTION

Chemical kinetics on fractals has been a tool for determining both the fractal and the spectral dimension of a given medium.<sup>1–4</sup> Conversely, such fractal media give rise to very "anomalous" laws of chemical kinetics, giving a new insight into heterogeneous kinetics.<sup>4–6</sup> Here a new method is described for distinguishing random from ordered fractal media or connected from disconnected ones ("dusts"). It is based on the early time difference in reaction rates between random and steady state distributions of reacting particles.<sup>7</sup>

Classically, chemical reactions depend on the initial (time = 0) reactant densities

( $\rho_0$ ) but not on the history of how such a density was achieved. For instance, a simple annihilation reaction ( $A + A \rightarrow 0$ ) will proceed as<sup>8</sup>:

$$\rho^{-1} - \rho_0^{-1} = kt \quad (1)$$

Recently this result has been generalized for fractal domain reactions<sup>4</sup>:

$$\rho^{-1} - \rho_0^{-1} = kt^f \quad (2)$$

where  $f$  is the random walk exponent ( $f = d_s/2$  where  $d_s$  is the spectral dimension). In both (1) and (2) only the overall initial density ( $\rho_0$ ) appears and not its detailed distribution.

The results described below show that  $\rho_0$  is not a sufficient criterion to determine the future reaction course in certain types of media. The same  $\rho_0$  originating in one case from a steady-state population and in another case from a pulse generated population will result in different relaxation characteristics (and times). This is shown below for both experimental systems and simulations. Specifically, naphthalene powders and naphthalene embedded in porous glass show the anomalous behavior in contrast to more homogeneous samples. Simulations on randomly disordered and linear lattices, or ordered fractals show similar anomalies, in contrast to crystalline lattices.

## EXPERIMENTAL

The naphthalene was purified by potassium fusion and zone refinement.<sup>9,10</sup> The crystals were mixed and grown by Klymko or his method.<sup>9,10</sup> Unsupported powdered naphthalene was prepared by grinding crystals in a mortar and pestle. The powder was immediately sealed between quartz plates and transferred to a cold (100 K) cryostat. Naphthalene was embedded in porous glass (Corning 7930 Vycor) by vacuum sublimation after cleaning the glass in boiling 30% hydrogen peroxide and rinsing with distilled water.<sup>3</sup>

The time dependence of naphthalene triplet-triplet annihilation was monitored by delayed fluorescence (340 nm), delayed excimer fluorescence (420 nm) and phosphorescence (500 nm), using bandpass interference filters in front of a photomultiplier tube placed directly against the cryostat's window. Currents from the photomultiplier were converted to a voltage with an operational amplifier and digitized with an analog to digital converter (Data Translation DT2805) in a Zenith Z-150 computer using ASYST software. Exciton pulses were initially created by mechanically shuttering the xenon arc lamp excitation through a monochromator, generally at 310 nm. The dependence of the relative rates and intensities of decay of the emission on initial excitation duration was examined. Steady state conditions were created by excitation over several seconds, while pulses lasting tens of milliseconds generated transient states. In general, the initial phosphorescence intensity at time zero resulting from steady state excitation was greater than that from pulses. For some studies, neutral density filters were added to the steady state

excitation until its resulting initial phosphorescence equaled that from unfiltered pulses. Alternatively, the filters were added until the initial delayed fluorescence intensities were equal for both modes of excitation. The light intensity at the sample was 3 microwatts. We estimate<sup>9</sup> an initial distance between triplet excitons of about 100 lattice distances (with a pulsed, "random" excitation). A result of about 130 is obtained based on the phototube output (0.01 volts) using the approach and parameters given by Klymko.<sup>9</sup>

## SIMULATIONS

The reaction  $A + A \rightarrow 0$  was simulated by random walks on a variety of lattice surfaces. At each step, the existing walkers were moved independently in a random direction.<sup>11</sup> Annihilation removes walkers when a reactant  $A$  moves to a lattice site occupied by another reactant  $A$ . Steady state conditions were generated by adding (at random locations) several new walkers per step until the total number of walkers was nearly constant. Although this may only have required several hundred steps, in general several thousand of these initial steps were taken. Pulsed conditions were then studied in a second simulation by adding in one step, to an initially empty lattice, the same number of walkers that exist at steady state. This produces an initial uniformly random distribution. In both cases, after stopping the addition of walkers, the number of walkers remaining (or number of reactants, equivalent experimentally to phosphorescence) was recorded for several thousand steps. The number of annihilations or reactions (reaction rate equivalent experimentally to delayed emission) at each step was determined as the difference between the number of walkers at that step and the next step. In order for the fluctuations or noise in this difference to be small, several hundred averages were performed. Additionally, moving point smoothing was performed. Generally, two new walkers were added per step, resulting in steady state concentrations under three percent. In some cases, blocked sites either at preselected or at random locations were introduced to restrict walker movement geometrically. Simulations on all clusters of randomly blocked lattices may produce isolated walkers unable to find others. To eliminate the resulting constant presence of those unreacting walkers, a "natural decay" lifetime was introduced, giving a small probability (0.04%) for each walker to be removed from the simulation at each step.

Some simulations were performed on pure square lattices with energy disorder.<sup>12</sup> Each lattice site location was randomly assigned an energy value. The distribution of these values was either even or skewed logarithmically towards high values. The probability of moving to a site of lower energy is the inverse of the number of possible movement directions (i.e. 0.25 for two dimensions). Movements to higher energy sites have this probability scaled (decreased) by the inverse of the exponential of the energy difference. Any remaining difference between unity and the sum of probabilities for moving over all directions is the chance that the walker does not move.

A special case of energy disorder is simulation with traps. Effectively there are only two energies, and walkers in the lower energy trap have zero probability of

moving, i.e. they are trapped. They may be removed by annihilation with a mobile walker.

A Zenith Z-241 computer was employed in Pascal.

## EXPERIMENTAL RESULTS

When using the same excitation intensity, all emissions of all samples at 6 K and 27 K exhibit decay rates from pulsed excitation that are relatively faster than those from steady state excitation, when both are scaled to the same maximum at time zero. Generally the pulse-created initial-intensity-peaks are lower than the steady-state ones. The faster decay of the pulsed excitation is *not* a result of lower initial exciton concentration since for delayed fluorescence the rate slows down as the illumination intensity (steady-state or pulsed) is decreased with neutral density filters (as expected).

The initial *steady state phosphorescence* intensities are higher than those from pulses indicating a higher number of excitons. When neutral density filters are added to the steady state excitation, to *equalize the initial phosphorescence*, the *pulsed delayed fluorescence emissions* have higher initial intensities and faster decay rates (Figures 1–5). The powdered naphthalene and naphthalene in Vycor glass results may be influenced by energetic as well as geometric disorder. The naphthalene fluorescence linewidth is about  $30\text{ cm}^{-1}$  for the powder and  $225\text{ cm}^{-1}$  for the Vycor glass sample (at 6 K). Energetic effects can be removed at higher temperatures. Since the differences described above still exist at 27 K, geometry appears to be the dominating factor. Energy disorder can also be reduced by using isotopically mixed single crystals. At low temperatures, exciton transport occurs on the

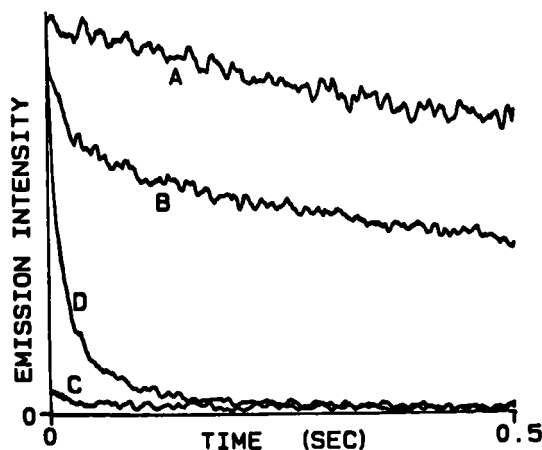


FIGURE 1 Emission decays from naphthalene in Vycor glass at 6 K following an excitation duration at 310 nm of: (A) and (C) 11 sec; (B) and (D) 55 msec. The excitation of (A) and (C) had a neutral density filter of 2.0 to equalize the initial phosphorescence intensity of (A) and (B). (A) and (B) show phosphorescence. (C) and (D) show delayed fluorescence on a different scale.

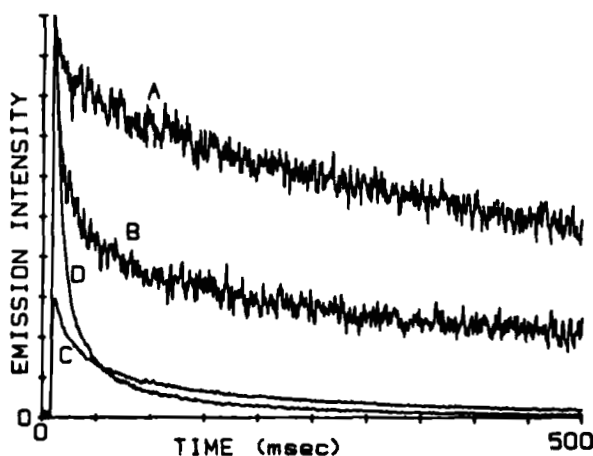


FIGURE 2 Same as Figure 1 for naphthalene powder. Conditions as in Figure 1 except neutral density filter of 1.2 for (A) and (C).

lower energy hydrogenated naphthalene while the higher energy deuterated molecules serve as geometric restrictions. The crystal face observed was the same for pulsed as for steady-state excitation. The 5% h8 in d8 naphthalene crystals show clear differences while the difference is much lower in 39% crystals (Figures 3–5). Above percolation (9% for these crystals) energy transfer is expected to resemble that in a single crystal.

Use of an excitation energy of 310 nm at naphthalene's absorption maximum may create a locally high concentration of triplets from pulsed excitation. Steady state excitation, because of the long triplet lifetime (2.1 sec), allows excitons to

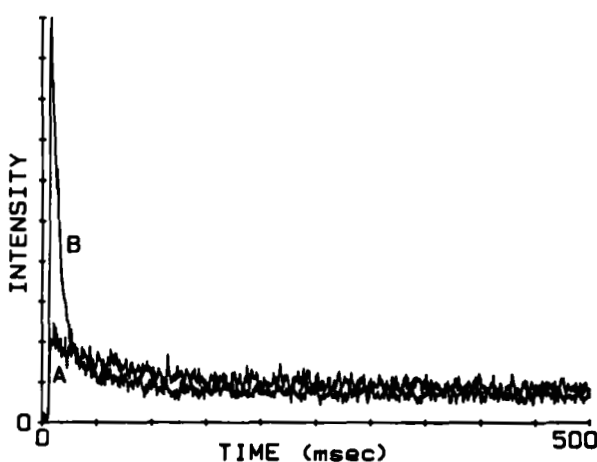


FIGURE 3 Delayed fluorescence decay from single crystal 5% naphthalene-h<sub>8</sub> in d<sub>8</sub> at 23 K following an excitation duration at 321 nm of: (A) 6 sec., neutral density filter = 1.5; (B) 30 msec, no neutral density filter. Note that the curves do cross.

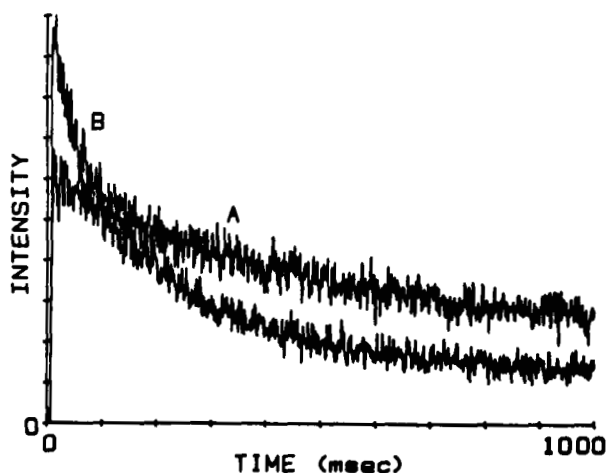


FIGURE 4 Same as Figure 3 except for 11% sample with neutral density filter of 1.8 for (A). Note that the curves do cross.

migrate away from the region in which they were created and to become more dilute. Thus, even though initial phosphorescence intensities may be equal, indicating equal numbers of excitons, the pulsed mode's concentration could be argued to be higher for this reason. This, then, could be argued to produce its faster decay rate. For this reason, an excitation energy as low as possible to still give decays with adequate signal-to-noise ratios was used so as to allow triplets to be created deeper into the sample. Wavelengths as high as 322 nm were sometimes possible. The absorption from lower wavelengths results in a deeper and more uniform excitation. Nevertheless, differences in the phosphorescence decays (triplet exciton density) (Figures 6, 7) and delayed fluorescence (decay rates) were still observed

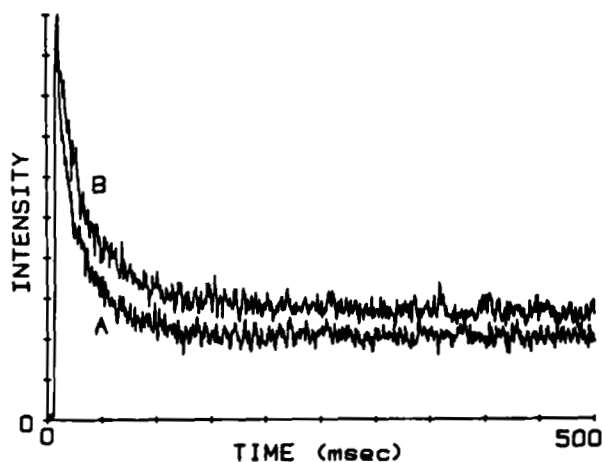


FIGURE 5 Same as Figure 3 except for 39% sample with neutral density filter of 1.0 for (A).

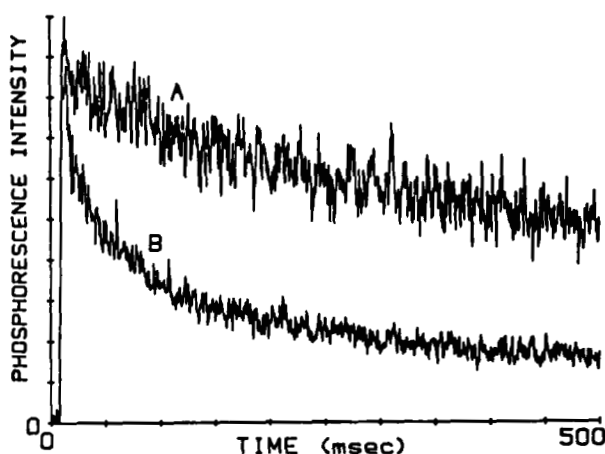


FIGURE 6 Naphthalene in Vycor glass phosphorescence as in Figure 1A and 1B, except excitation at 322 nm and neutral density filter of 1.7 for (A).

when this was done with steady-state and pulsed excitations. Thus the penetration depth of the exciting radiation is not a major factor in our results.

Spectra of the disordered naphthalene samples exhibit emission from excimers. The excimer intensity, relative to fluorescence, increases with temperature. However, the delayed fluorescence and phosphorescence decays given in Figures 1 and 2 do not include excimer contributions (and there are none for single crystals).

## SIMULATION RESULTS

For three-dimensional perfect lattices, decays resulting from steady state and pulsed generation of reactants are similar, as expected classically (see below). However,

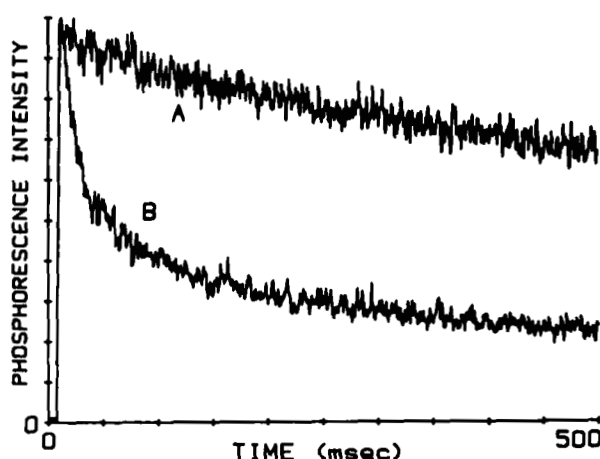


FIGURE 7 Naphthalene powder phosphorescence as in Figure 2A and 2B except excitation at 322 nm and neutral density filter of 1.3 for (A).



differences appear with the introduction of random blocked sites and become significant at active site concentrations *below* 50% (Figure 8). In these latter simulations the lattices include finite clusters. The decay rate of pulsed reactants is faster than steady state reactants of the same initial concentration. The number of reactions (reaction rate) for pulsed excitation also decreases more rapidly and has a higher initial number of reactions at step one (time zero) than for steady state excitation. Note that the number of reactions is a measure of the instantaneous rate of reaction. [It is possible for this parameter to decay relatively slowly yet maintain a high value which is indicative of a very rapid reaction.] To compare different three-dimensional topologies we plot (Figure 9) the *ratios* of random (pulsed) excitation rates over steady-state rates for the binary lattice (see above), the perfect lattice and the Menger sponge.<sup>13</sup>

In contrast to simulations on three-dimensional perfect lattices, two-dimensional perfect lattices do exhibit (Figure 10) small differences in the two decay rates at early steps (times). The difference increases with decreasing active site concentration, becoming significant *below* 70%. At 60% active sites, when the simulated reaction is performed on only the largest connected cluster contacting opposite lattice sides (percolating maxi-cluster), the differences are smaller than for the same concentration but including all clusters, yet larger than for a perfect lattice.

The importance of the role of the blocked sites during walker creation and during decay can be demonstrated. If blocked sites are present for the *duration* of the steady state or pulsed walker creation but are removed (at time  $t = 0$ ) for the decay so that the decay occurs on a perfect lattice, then the degree of difference between the steady state and pulsed decays is equal to that produced when the

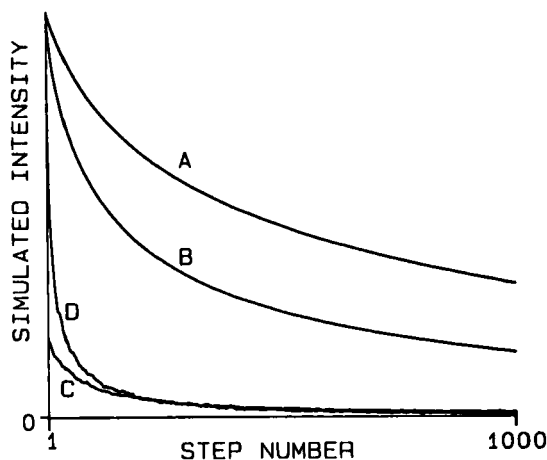


FIGURE 8 Simulation of  $A + A \rightarrow 0$  for 1000 decay steps on *all* available clusters of a 40% guest site  $35 \times 35 \times 35$  cube, following two methods of creating the initial reactant distribution. (A) and (C) are for steady state (after 2000 steps of adding 2 reactants/step). (B) and (D) are for a random pulse, i.e. randomly adding (at step number zero) the same number of reactants existing at step number zero of the (A) or (C) decay. (A) and (B) show the number of reactants remaining, analogous experimentally to phosphorescence intensity. (C) and (D) show the reaction rate, analogous experimentally to delayed fluorescence intensity, on a different scale.

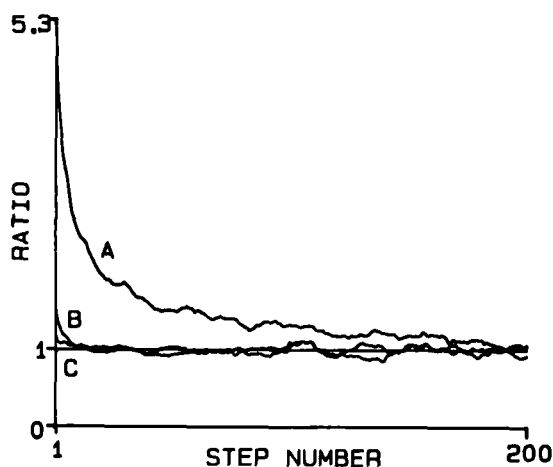


FIGURE 9 (A) Ratio of Curve D to Curve C in Figure 8; (B) Same as (A) except on a third order Menger sponge; (C) Same as (A) except on a 100% guest site cube.

entire simulation occurs on a perfect lattice. That is, in three dimensions there is no difference; in two dimensions there is very little difference. The reaction is no longer sensitive to its history. This indicates that the difference in decays is not merely due to different reactant distributions. Although removing the blocked sites increases the dimensionality which makes the reaction less sensitive to reactant distributions, an effect should still be observed, as discussed later for stirred reactions.

Alternatively, the walkers can be created on a perfect lattice and allowed to

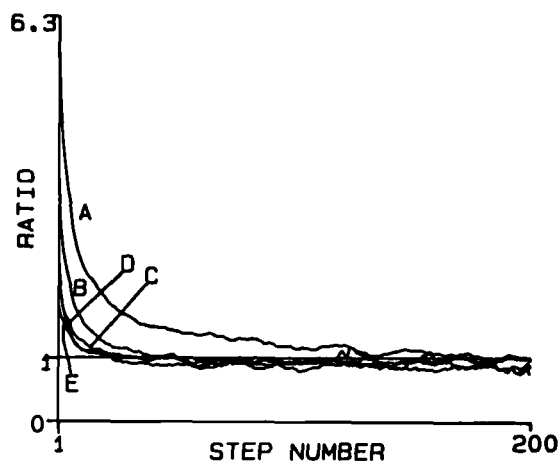


FIGURE 10 Ratio of pulsed to steady state creation *reaction rate*, as in Figure 9 except: (A)  $200 \times 200$  square lattice with 60% guest sites (all clusters); (B) Same as (A) but on the percolating maxicluster only; (C) Seventh order Sierpinski gasket; (D) Fifth order Sierpinski carpet; (E) Same as (A) but with 100% guest sites.

decay in the presence of randomly blocked sites. Again, no differences are observed between this model and simulations done entirely on a perfect lattice. Thus it is necessary to have blocked sites initially to affect the reactant distribution at creation time. In addition, these blocked sites are responsible for restricting the transport during the decays.

The dependence of the degree of difference between steady state and pulsed decays on the number of steady state steps taken was examined. For a two-dimensional 60% active site percolating maxi-cluster on a  $200 \times 200$  square lattice with approximately 12,000 active sites, steady state is reached after 250 steps of adding 2 walkers per step. The respective decay rates do not change whether 250 or 2,000 steady state steps are initially taken. Thus once a steady state (in the number of walkers) is reached the factors influencing the difference in decay rates are already fully effective.

The differences in decay rate resulting from steady state and pulsed generation of reactants are not merely due to the existence of blocked sites. On a Menger sponge (a periodic three-dimensional ordered fractal), decay rates for the two generation methods are nearly identical (Figure 9). (The same was found for a perfect unblocked three-dimensional cube (Figure 9)). This occurs in spite of the fact that the third order Menger sponge has only 41% active sites. The rates of decay (Figure 10) on a Sierpinski carpet (the same topology as a Menger sponge but in two dimensions) are in-between those of a perfect two-dimensional lattice (Figure 10) and a percolating maxi-cluster (Figure 10).

These simulations were performed without moving walkers whose "proposed" direction to move would take it to a blocked site but still counting such a "proposal" as a step (blind or non-forced walk).<sup>14</sup> For the two-dimensional maxi-cluster, Sierpinski carpet or Menger sponge, the proposed direction to move can repeatedly randomly chosen until it moves the walker to a site either empty or occupied by another walker, but not blocked, so that there is a real move at each step (myopic or forced walk).<sup>14</sup> If this is done, the decay rates increase slightly relative to non-forced walks but the degree of difference between steady state and pulsed decays are the same. This increase is expected as the walkers do not waste steps attempting to move to blocked sites.

The largest differences between steady state and pulsed decays occurs on a perfect one-dimensional line (Figure 11). The number of reactions at step one from pulsed generation is *eight times* as large as from steady state (Table I). It then rapidly decreases to approximately that of steady state creation. This is a result of a relatively large decrease in the number of reactants at very early steps. In contrast to two or three dimensions containing blocked sites, the differences on an unblocked one-dimensional line cannot be caused by peculiar transport effects in restricted geometries, but must instead be due to variations in the initial reactant distribution. The initially faster, pulsed reaction rate means that more of its created walkers are in close proximity to one another at "step one" than for the steady state creation. During the process of steady state excitation, walkers that were near each other would have found one another and annihilated (at  $t < 0$ ). Thus, their average separation is greater than for the pulsed generation and more steps are required to find each other. The creation of all the walkers in one pulsed step contains no

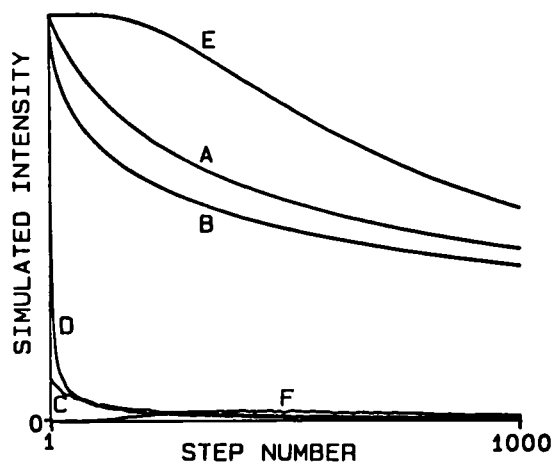


FIGURE 11 (A, B, C, and D) Same as Figure 8, except on a 100% guest site one dimensional line of length 30,000. Curve (E) and (F) are the number of reactants and reaction rate, respectively, for an initially uniform (superlattice) distribution: one particle at every 50-th lattice site.

restrictions on the allowed locations and so some will be created near each other. There are about ten times as many walker pairs created one lattice unit apart from a pulse than from steady state. The functional form of the distribution of the reactant separations ( $x$ ), at  $t = 0$ , is exponential (Poissonian) for the pulsed (uniformly random) excitation in one dimension ( $e^{-ax}$ ). However, the steady-state distribution has a different functional form: a skewed exponential ( $xe^{-bx}$ ), at least to first order, for the  $A + A \rightarrow 0$  reaction and a still different functional form for  $A + A \rightarrow A$ . These non-random distributions are presently an active frontier in reaction kinetics.<sup>6,15,16</sup>

TABLE I

Ratio of the number of annihilation events (reaction rate) resulting from pulsed reactant creation compared to steady state for the simulation  $A + A \rightarrow 0$  on various lattices. Values are for the first step following the end of creation.

Lattice	Ratio
<i>3-dim</i>	
40% guest (all clusters)	5.25
Menger sponge	1.56
100% guest	1.21
Islands ( $3 \times 3 \times 3$ )	4.25
<i>2-dim</i>	
60% guest (all clusters)	6.28
60% guest (percolating maxi-cluster)	3.95
Sierpinski gasket	2.59
Sierpinski carpet	2.51
100% guest	1.85
<i>1-dim</i>	
100% guest	8.06
Islands (20 sites)	18.0

These effects should also be present in two or three dimensions without blocked sites and should lead to similar differences. However, the lower dimensionality (fewer additional directions of movement) in one dimension increases the probability of annihilation of two walkers initially near each other. A walker one lattice unit away from another has a 50% chance of annihilating in the next step in one dimension but only 17% in the three-dimensional cubic lattice.

The differences resulting from these excitation effects can be made even more dramatic by randomly regenerating the locations of all of the walkers that exist at the end of each step before taking the next step. In effect, then each step acts as if its walkers were created from a pulse instead of just the first step. This is the so-called stirred model.<sup>14</sup> The reaction rate of all pulsed simulation conditions studied increase in the stirred mode, with the greatest increase being in one-dimension for reasons just described above.

Regenerating the walker's locations at the end of each step means that the reaction can occur only from walkers created one lattice unit from each other. Because a random pulsed distribution appears to create a significant number of walkers located within one step of each other, it is of interest to extend this idea to examine the *number of steps that a walker exists between its creation and its annihilation* for reacting systems at steady state. Figure 12 shows the *existence lifetime distribution* of walkers at steady state on a perfect three dimensional cube and on a one-dimensional lattice. The most probable existence lifetime is only one step (as is the case for all dimensions, with or without blocked sites). For the cubic lattice the monotonically decaying distribution is exponential (except for the first 25 steps) with a "lifetime" of 112 steps based on a logarithmic fit over a wide region (see Figure 12A). As the dimensionality decreases or the geometric disorder increases, the fraction of walkers with a lifetime of only one step increases. However,

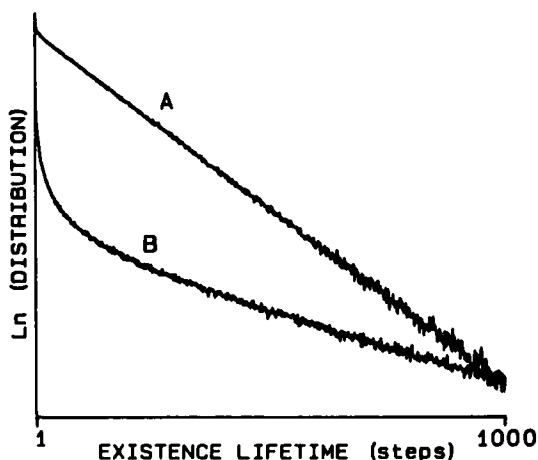


FIGURE 12 Logarithm of the distribution of the number of steps a walker exists between its creation and annihilation ( $A + A \rightarrow 0$ ) at steady state of adding two walker/step on: (A) a 100% guest site  $35 \times 35 \times 35$  cube and (B) a 100% guest site one-dimensional line of length 30,000.

so does the maximum (longest) lifetime. Also, the fit to an exponential begins at longer lifetimes (Figure 12B).

A 100% active solid square rod exhibits cross-over behavior from one to three dimensions as the side-width increases from one. Non-cyclic side boundary conditions were used and a walker located on a side wall that tried to move outside the rod was forced to choose another direction. As the width was increased, the length decreased to keep the number of available sites constant at 30,000. As the width increases, the difference between steady-state and pulsed decay rates becomes smaller. Above the width of 10, the behavior is the same as for a perfect cube.

The presence of energy disorder on lattices containing no geometric disorder (100% active sites) was not found to produce differences in decay rates above that observed without energy disorder. Traps, however, produce significant differences. In two dimensions the effect becomes noticeable above a trap concentration of 0.2%; in three dimensions, above 0.1%. At 1% traps, about half the walkers are trapped at steady-state and the decay rate of the walker density is significantly slower than for pulsed generation or for steady state generation without traps (Figure 13).

## DISCUSSION

The differences in decay rates observed experimentally can be simulated under the appropriate lattice conditions. From comparison of the behavior with randomly blocked sites vs. ordered fractals, random disorder appears to be a necessary condition for our effect (except in one dimension). At steady state, walkers in large open areas have been mostly annihilated while relatively more of them survive in the small isolated regions. In contrast, adding all of the walkers in one step produces a distribution with a relatively higher representation in the open areas. Walkers in

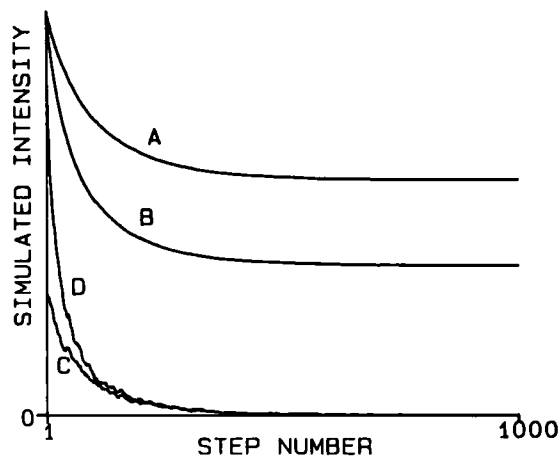


FIGURE 13 Same as Figure 8, but on a 100% guest site cube with 1% traps.

such regions find each other quickly and produce a more rapid initial decay rate. As all regions are similar in the ordered fractals, walkers cannot become really isolated in areas where their movement is relatively more restricted.

Lattices without geometric disorder but with energy disorder should also serve to *isolate more walkers* in regions where their movement is restricted *at steady state*, compared to pulsed generation. The lack of an effect with the energy disorders employed here is most likely due to a significant probability of escape from low energy sites, i.e. the effective temperature is high. When the probability is made zero through the use of traps, large effects are observed.

Powdered naphthalene represents a microcrystalline sample whose outer and inner surfaces are perturbed, while the Vycor sample consists of interconnected regions with a mean pore size of about 40 Angstroms. Powdered and isotopically mixed single crystal naphthalene could be simulated geometrically by "all clusters on the randomly blocked lattices" while the Vycor sample is best described by a solid rod (or hollow tube if the naphthalene concentration is not high enough to completely fill the pores).

The annihilation rate dependence on the history of reactant generation can be used to probe the randomness of disordered structures. Different regions of the structure are probed with a different weight as the excitation pulse-width is varied. This may prove a valuable method for characterizing pore sizes and their distributions.<sup>3,17</sup> Such work is currently in progress.

We have argued before,<sup>3,7</sup> based on a different kind of kinetic parameter (the heterogeneity exponent for *long* time decays), that naphthalene channels in porous Vycor are quasi-one-dimensional. Our present kinetic data (based on local densities at *early* decay times) appear to be consistent with the above picture and with other work.<sup>18</sup> This can also be seen qualitatively by comparing curves C and D of Figures 1 and 11. More importantly, our general argument that the high value of the heterogeneity exponent ( $h > 0$ ,  $h \approx 0.5$ ) is characteristic of low effective (spectral) dimensions is certainly borne out here. Previous mixed crystal data<sup>9,10</sup> showed a heterogeneity factor that is increasing below 12% naphthalene ( $C_{10}H_8$  in  $C_{10}D_8$ ) alloy concentrations (while above that  $h = 0$ ). Again we see here a qualitative difference between the high concentration sample (39%) and the low concentration alloys (at or below long-range percolation<sup>9,10,19</sup>). The local density (early decay time) kinetic effect is thus a new criterion for the characterization of sample heterogeneity [we include low dimensionality as a special case of heterogeneity]. We further note that the exciton transport in these samples is incoherent (hopping).<sup>19</sup> A coherent transport would give different results. Obviously there is no mixing (stirring) mechanism available for our exciton ensembles. Homogeneous chemical kinetics implies efficient stirring (convection) and thus no local density effects. However, it is interesting to see that diffusion-caused "self-stirring"<sup>14</sup> is sufficient to effectively quench the local density effect in the "homogeneous" lattices (simple cubic—Figure 9, as well as square lattice and others—Figure 10). Thus, exciton hopping in perfect (non-alloy) crystals is not expected to show the local density effect. Indeed, it is not observed.

This new effect may also enable one to calibrate the absolute number of random hopping events within a given time period. The simulations indicate that the reaction

rate ratio (equivalent experimentally to the *delayed fluorescence ratio*, Figures 9,10) reaches unity after roughly  $10^3$  "steps." Experimentally, this ratio of unity is achieved after about 1 sec. This gives an average hopping time of about 1 ms.. Furthermore, assuming effective one-dimensional topology, this gives a mean number of distinct sites visited by the excitation of about  $10^2$  which is consistent with recent work.<sup>3,20,21</sup>

We notice that in our simulations the pulse-created sample is truly random while in the experiment the pulse duration is often of the order of the fluorescence decay (though the phosphorescence is mostly longer). Ideally, the pulse duration should be much shorter. Presently, experiments are being conducted in our laboratory with nanosecond pulses (excimer lasers). This also helps to increase the initial exciton density and bring it closer to the simulation densities (lower density simulations need higher computing power). Also, some of the samples have been investigated recently over larger temperature ranges. This seems to bear out our implicit assumption that triplet polarization, due to spin-selection (in the process of annihilation,<sup>22,23</sup> does not play an important role in the observed difference between pulsed and steady-state excitation. (It would be interesting, however, to study magnetic field effects, especially at low temperatures). The temperature studies also confirm that trapping by defects, and heterofusion at defects, are not of major concern. We note here that the samples studied in this work have been selected on the basis of previous studies<sup>3,10,15,16</sup> showing domination by the homofusion process (in contrast to other samples, where trapping and heterofusion dominate.<sup>3,16,21</sup> Overall, while improvements in both experimental procedures and computer simulations may lead to better quantitative comparisons, the present results do establish the importance of initial conditions and their potential for the study of sample morphology and excitation kinetics.

We expect similar local density effects to appear in many analogous solid-state and "physical" reactions: Electron-hole recombination, defect annihilation or aggregations, and soliton-antisoliton annihilation. The same should be true for diffusion-limited solid-state and surface chemical reactions.

## Acknowledgment

Supported by NSF Grant DMR 88-01120

## References

1. J. Klafter, A. Blumen and G. Zumofen, *J. Stat. Phys.*, **36**, 56 (1984).
2. W. D. Dozier, J. M. Drake and J. Klafter, *Phys. Rev. Lett.*, **56**, 197 (1986).
3. R. Kopelman, S. J. Parus and J. Prasad, *Phys. Rev. Lett.*, **56**, 1742 (1986).
4. R. Kopelman, *J. Stat. Phys.*, **42**, 185 (1986).
5. J. Prasad and R. Kopelman, *J. Phys. Chem.*, **91**, 265 (1987).
6. R. Kopelman, *Science*, **241**, 1620 (1988).
7. R. Kopelman and S. J. Parus, in *Fractal Aspects of Materials II*, eds. D. W. Schaefer *et al.*, (Materials Research Society, Boston, 1986), p. 50.
8. P. W. Atkins, *Physical Chemistry*, (Freeman, San Francisco, 1978).
9. P. W. Klymko, Ph.D. Thesis, University of Michigan, Ann Arbor (1984).
10. P. W. Klymko and R. Kopelman, *J. Phys. Chem.*, **87**, 4565 (1983), and references therein.



11. R. Kopelman, J. Hoshen, J. S. Newhouse and P. Argyrakis, *J. Stat. Phys.*, **30**, 355 (1983).
12. L. W. Anacker, R. Kopelman, *Phys. Rev.*, **B29**, 511 (1984); P. Argyrakis and R. Kopelman, *J. Phys. Chem.*, **91**, 2699 (1987).
13. B. B. Mandelbrot, *The Fractal Geometry of Nature*, (W. H. Freeman, San Francisco, 1983).
14. P. Argyrakis and R. Kopelman, *Phys. Rev.*, **B29**, 511 (1984); P. Argyrakis and R. Kopelman, *J. Phys. Chem.*, **91**, 2699 (1987).
15. S. J. Parus and R. Kopelman, *Phys. Rev.*, **A39**, 889 (1989).
16. R. Kopelman, S. J. Parus and J. Prasad, *Chem. Phys.*, **128**, 209 (1988).
17. D. L. Johnson, J. Koplik and L. M. Schwartz, *Phys. Rev. Lett.*, **57**, 2564 (1986).
18. D. W. Schaefer, B. C. Bunker and J. P. Wilcoxon, *Phys. Rev. Lett.*, **58**, 284 (1987).
19. R. Kopelman, in *Modern Problems in Solid State Physics*, vol. 4, eds. V. M. Agranovich and R. M. Hochstrasser, (North-Holland, Amsterdam, 1983), p. 139.
20. R. Kopelman, L. Li, S. J. Parus and J. Prasad, *J. Lumin.*, **38**, 289 (1987).
21. J. Prasad and R. Kopelman, *Phys. Rev. Lett.*, **59**, 2103 (1987).
22. M. Pope and C. E. Swenberg, *Electronic Processes in Organic Crystals*, (Clarendon, Oxford, 1982).
23. C. E. Swenberg and N. E. Geacintov, in *Organic Molecular Photophysics*, vol. 1, ed. J. B. Birks (Wiley, New York, 1973).